HHS Public Access

Author manuscript

Oncogene. Author manuscript; available in PMC 2010 November 20.

Published in final edited form as:

Oncogene. 2010 May 20; 29(20): 2962–2972. doi:10.1038/onc.2010.67.

Imatinib-resistance associated with BCR-ABL upregulation is dependent on HIF-1α-induced metabolic reprogramming

Fangping Zhao[1], **Anthony Mancuso**[1], **Thi V. Bui**[1], **Xuemei Tong**[1], **Joshua J. Gruber**[1], **Cezary R. Swider**[2], **Patricia V Sanchez**[2], **Julian J. Lum**[3], **Nabil Sayed**[1], **Junia V. Melo**[4], **Alexander E. Perl**[2], **Martin Carroll**[2], **Stephen W. Tuttle**[5], and **Craig B. Thompson**[1,6]

[1]Department of Cancer Biology, Abramson Cancer Center, University of Pennsylvania School of Medicine, Philadelphia, Pennsylvania, USA

[2]Hematology-Oncology Division, Department of Medicine, University of Pennsylvania School of Medicine, Philadelphia, Pennsylvania, USA

[3]Deeley Research Centre, BC Cancer Agency, Victoria, B.C. Canada

[4]Institute of Medical and Veterinary Science, Adelaide, South Australia, Australia

[5]Department of Radiation Oncology, University of Pennsylvania School of Medicine, Philadelphia, Pennsylvania, USA

Abstract

As chronic myeloid leukemia (CML) progresses from the chronic phase to blast crisis, the levels of BCR-ABL increase. In addition, blast transformed leukemic cells display enhanced resistance to imatinib in the absence of BCR-ABL resistance mutations. Here we show that when BCR-ABL transformed cell lines were selected for imatinib resistance *in vitro*, the cells that grew out displayed higher BCR-ABL expression comparable to increase seen in accelerated forms of the disease. This enhanced expression of BCR-ABL was associated with an increased rate of glycolysis but a decreased rate of proliferation. The higher level of BCR-ABL expression in the selected cells correlated with a non-hypoxic induction of HIF-1α that was required for cells to tolerate enhanced BCR-ABL signaling. HIF-1α induction resulted in an enhanced rate of glycolysis but reduced glucose flux through both the TCA cycle and the oxidative arm of the pentose phosphate pathway (PPP). The reduction in oxidative PPP mediated ribose synthesis was compensated by the HIF-1α-dependent activation of the non-oxidative PPP enzyme, transketolase, in imatinib-resistant CML cells. In both primary cultures of cells from patients exhibiting blast transformation and *in vivo* xenograft tumors, use of oxythiamine which can inhibit both the pyruvate dehydrogenase complex and transketolase resulted in enhanced imatinib sensitivity of tumor cells. Together, these results suggest that oxythiamine can enhance imatinib efficacy in patients that present in the accelerated form of the disease.

[6]Correspondence: craig@mail.med.upenn.edu; FAX 215-746-5511.

Keywords

imatinib (gleevec, STI571); resistance; HIF-1α; pentose phosphate pathway; glucose metabolism; cell survival

Introduction

Imatinib (gleevec, STI-571) is a small molecule that targets the BCR-ABL tyrosine kinase and is effective in the treatment of BCR-ABL positive chronic myeloid leukemia (CML). While imatinib has been remarkably successful in reducing the tumor burden and suppressing the progression of patients in the chronic phase of CML, it has been less successful in the treatment of the accelerated phase of the disease. Although point mutations in the ABL kinase domain appear to be the main cause of secondary resistance to imatinib, such point mutations do not appear to account for all of the resistance observed in patients with the accelerated form of CML (Gorre *et al.*, 2001; Khorashad *et al.*, 2006; O'Hare *et al.*, 2006; Sherbenou and Druker, 2007). One correlation that has been observed in leukemic samples from untreated patients as the disease progresses is increased expression of BCR-ABL. This has led to the speculation that the amount of BCR-ABL expressed by the tumor cells contributes to the sensitivity of the cells to imatinib (Keeshan *et al.*, 2001; Barnes *et al.*, 2005a; Modi *et al.*, 2007). Whether the increase in BCR-ABL simply requires a higher level of imatinib to suppress or induces more qualitative changes in intracellular signaling pathways leading to imatinib-resistance has not been examined.

BCR-ABL transformation is associated with cell-autonomous proliferation and increased glucose metabolism (Barnes *et al.*, 2005b; Modi *et al.*, 2007; Kominsky *et al.*, 2009). The effects of BCR-ABL on glucose uptake exceed the metabolic needs of the cells and the excess glucose carbon is secreted from the transformed cells in the form of lactate. This metabolic conversion in a cell capable of oxidative phosphorylation is termed aerobic glycolysis or the Warburg effect. Recently, we demonstrated in non-transformed cells that when growth factor-induced glucose uptake exceeded cellular needs, the cells underwent an induction of HIF-1α (Lum *et al.*, 2007). The consequent HIF-1α-mediated reprogramming of glucose metabolism directs glycolytic pyruvate away from the mitochondria, converting it to lactate that is secreted from the cell (Lum *et al.*, 2007). The consequence of this growth factor-induced non-hypoxic induction of HIF-1α is that the resulting metabolic reprogramming leads to a loss of ribose produced by oxidative arm of the pentose phosphate pathway and TCA cycle intermediates required for the macromolecular synthesis and an impaired ability to proliferate. Whether similar changes occur during oncogene-induced aerobic glycolysis has not been investigated.

Recently, we and others have observed that BCR-ABL transformed cells that survived in the presence of continuous imatinib treatment displayed higher levels of BCR-ABL expression (Mahon *et al.*, 2000). In this report, we demonstrate that imatinib-resistant cells displayed increased aerobic glycolysis but decreased proliferation *in vitro*. While the BCR-ABL tyrosine kinase activity could still be repressed by imatinib, pharmacologically relevant concentrations of imatinib failed to suppress cell proliferation. These results confirmed that

the resistant cell lines lacked BCR-ABL mutations to confer imatinib resistance and suggested that the activation of compensatory pathways may be involved in maintaining the ability of the cells to survive and proliferate in the presence of imatinib. The increased glycolysis and decreased cell proliferation in resistant cells were both found to depend on the non-hypoxic activation of HIF-1α. HIF-1α induction also shifted ribose synthesis preferentially to the non-oxidative arm of the PPP. Oxythiamine as an inhibitor of the thiamine dependent enzymes in both the TCA cycle and non-oxidative pentose phosphate pathway could restore imatinib sensitivity in resistant cells *in vitro*. Combination therapy with oxythiamine and imatinib led to a synergistic reduction of *in vivo* growth of both imatinib-sensitive and imatinib-resistant tumor xenografts. In addition, oxythiamine enhanced the efficacy of imatinib in primary CML cells isolated from patients in the accelerated/blastic phase of the disease. Together, the data suggests that the induction of HIF-1α in cells exhibiting a high level of BCR-ABL-induced glucose uptake contributes to their imatinib resistance.

Results

Imatinib-resistant cells have upregulated BCR-ABL protein level, increased glucose uptake, and reduced cell proliferation

To obtain cells that can survive persistent exposure to imatinib, BCR-ABL-transformed murine hematopoietic BaF3 cells (BaF3/p210) (Carroll *et al.*, 1997) were continuously cultured in 500 nM imatinib (Deininger *et al.*, 2005; Dewar *et al.*, 2005) until the outgrowth of a resistant population was obtained. To confirm their imatinib-resistance, the selected cells along with isogenic non-selected cells were treated with varying concentrations of imatinib for 2 days and cell proliferation was measured. Sensitive cells displayed a dose-dependent suppression of proliferation while resistant cells were unaffected over the same dose range (Figure 1a and Supplemental Figure 2a). In contrast to the lack of change in proliferation and viability in cells expressing the mutant form of BCR-ABL (T315I) (Supplemental Figure 1a and 1b (Gumireddy *et al.*, 2005), higher concentrations of imatinib inhibited cell proliferation and induced cell death in a dose-dependent fashion, suggesting that these cells selected for imatinib resistance still rely on BCR-ABL for their survival and proliferation. Consistent with their ability to continue to proliferate in the presence of imatinib at 500nM, resistant cells maintained residual BCR-ABL activity, as shown by auto-tyrosine phosphorylation (Figure 1b). Transient withdrawal of imatinib from culture led to a de-repression of BCR-ABL kinase activity in resistant cells as evidenced by tyrosine phosphorylation and STAT5 phosphorylation (Figure 1b). Therefore, resistant cells do not revert to the phenotype of imatinib-sensitive cells upon imatinib withdrawal and instead retain increased BCR-ABL levels.

Metabolic profiling revealed that the resistant cells had a significantly higher glycolytic rate and their glucose consumption was not suppressed by imatinib, as compared to isogenic sensitive cells over the same dose range, although higher doses eventually caused decreased glucose consumption (Figure 1c). In contrast to this, cells expressing the mutant form of BCR-ABL (T315I) did not demonstrate any change in glucose metabolism when high doses of imatinib was present in the culture (Supplemental Figure 1c). Despite increased glucose

metabolism, the resistant cells showed a reduced proliferation rate in comparison to isogenic sensitive cells. This reduced proliferation was observed when the cells were cultured in the presence or absence of imatinib (Figure 1d). When resistant and sensitive cells were co-cultured in the absence of imatinib, the sensitive cells consistently outcompeted the resistant cells (data not shown).

We also obtained a human CML cell line similarly selected for imatinib resistance, LAMA-84-R (LR) (Mahon *et al.*, 2000). Consistent with observations in murine resistant cells, human resistant cells did not show suppression of either cell proliferation or glucose consumption when exposed to a range of imatinib doses that resulted in the suppression of the growth of isogenic control cells (Figure 1e, 1g and Supplemental Figure 2b). Imatinib resistant cells in the presence of imatinib at the physiological concentration (1000 nM) demonstrated residual BCR-ABL kinase activity, as demonstrated by STAT5 phosphorylation (Figure 1f). However, upon withdrawal of imatinib from resistant cells, increased BCR-ABL downstream signaling was observed, in comparison to isogenic control cells as indicated by STAT5 phosphorylation. As with the murine cells, human imatinib-resistant cells also displayed increased glucose consumption rate, in comparison to isogenic control cells at all doses of imatinib tested (Figure 1g). However, imatinib over 2000 nM led to sharp reductions in glucose consumption and cell proliferation in resistant cells. In addition, slower cell proliferation was observed in human imatinib-resistant cells as compared to sensitive cells (Figure 1h).

Imatinib-resistant cells display activation of HIF-1α

When the glucose uptake of growth factor-stimulated cells exceeds the capacity of the cells to assimilate glucose, the resulting mitochondrial ROS leads to an induction of HIF-1α that is required to allow cells to secrete excess glycolytic pyruvate as lactate (Pelicano *et al.*, 2006; Bell and Chandel, 2007; Lum *et al.*, 2007; Pan *et al.*, 2007). Although this induction of HIF-1α promotes cell viability, it results in a paradoxical increase in glucose metabolism and a reduction of cell proliferation (Lum *et al.*, 2007). Because the imatinib-resistant cells exhibited such a phenotype, we examined the expression of HIF-1α. Induction of HIF-1α at both mRNA and protein levels was observed under normoxic conditions in both the murine and human BCR-ABL transformed cell lines selected for imatinib resistance (Figure 2). In addition, induction of multiple HIF-1α targets at the mRNA and/or protein levels was observed in resistant cell lines, including vascular endothelial growth factor A (VEGFA), phosphoglycerate kinase 1 (PGK1), pyruvate dehydrogenase kinase 1 (PDK-1) and pyruvate kinase M2 isoform (PKM2) (Figure 2b, 2d and Supplemental Figure 3).

Imatinib-resistant cells have increased glucose flux for ribose synthesis through the non-oxidative arm of the PPP

One potential mechanism by which HIF-1 induction affects cell growth is through its ability to impair TCA cycle flux and reduce glucose flux through the oxidative pentose phosphate pathway (Gupte and Wolin, 2006; Tuttle *et al.*, 2007). However, hypoxia induces both PKM2 and transketolase (Tkt) (Kress *et al.*, 1998; Haseloff *et al.*, 2006). Since we observed the non-hypoxic induction of HIF-1α in imatinib-resistant cells, we sought to determine if there was also an induction of PKM2 and Tkt in the resistant cells that resulted in increased

glycolytic flux through the non-oxidative PPP. Expression of both PKM2 and transketolase family genes was found to be elevated in resistant cells and resistant cells exhibited increased transketolase activity (Figure 2, 3a and Supplemental Figure 3).

In order to measure the relative contribution of the oxidative and the non-oxidative PPP to ribose synthesis, we established a ^{14}C tracing assay to monitor the incorporation of glucose carbon into ribose (Supplemental Figure 4). Based on reactions in the PPP (Katz and Rognstad, 1967), ^{14}C incorporation into RNA from [1-^{14}C]-glucose (glucose labeled at carbon 1) was used as an indicator of ribose derived from the non-oxidative arm and that from [6-^{14}C]- glucose was used as an indicator of ribose derived from both the oxidative and non-oxidative arms of the PPP. The ratio of ^{14}C-RNA CPM from the two isotopes ([1-^{14}C]/[6-^{14}C]) was used as an index of the relative level of RNA synthesized through the non-oxidative arm of the PPP (TKT flux). As shown in Figure 3b, imatinib-resistant cells exhibited a relative 40% increase in TKT flux, compared to isogenic-sensitive cells. This change was a result of both an increase in glucose flux into RNA *via* the non-oxidative arm and a decreased flux into RNA through the oxidative arm of the PPP. The decrease in glucose flux through the oxidative arm of the PPP in resistant cells was further confirmed by $^{14}CO_2$ released from [1-^{14}C]-glucose (Figure 3c). In addition, a reduction in glucose flux through the TCA cycle was observed, as measured by $^{14}CO_2$ release from [6-^{14}C]-glucose in resistant cell lines (Figure 3d for BR and data not shown for LR). The reduction in TCA cycle activity correlated with the induction of pyruvate dehydrogenase kinase-1 (PDK-1) upon HIF-1α activation (Supplemental Figure 3c) (Kim *et al.*, 2006; Papandreou *et al.*, 2006).

Induction of HIF-1α is sufficient to direct glucose-mediated ribose synthesis preferentially through the non-oxidative arm of the PPP

To study if activation of HIF-1 plays a role in regulating the pentose phosphate pathway, BCR-ABL transformed imatinib sensitive cells were cultured under hypoxic conditions (0.5% oxygen) for 2 days before ^{14}C labeled glucose was added to the cell culture to evaluate the relative TKT flux for ribose synthesis. As shown in Figure 4a, cells under hypoxic conditions demonstrated a significant induction of non-oxidative PPP for their ribose synthesis, as a result of an increase in the transketolase mediated non-oxidative ribose synthesis and a reduction in G6PD mediated ribose synthesis. To further address if HIF-1α is sufficient to promote glucose flux through the non-oxidative PPP for ribose synthesis, we used 293T cell lines stably transfected with either vector or a non-degradable *HIF-1α* construct (HIF1A-DPA) in an inducible system (Hu *et al.*, 2003) (Figure 4b). Compared to vector-transfected cells, cells with HIF-1α induction demonstrated a 90% decrease in glucose flux in the TCA cycle, as measured by $^{14}CO_2$ release from [6-^{14}C]-glucose (Figure 4c), as previously reported by others (Kim *et al.*, 2006; Papandreou *et al.*, 2006). Cells with HIF-1α induction also showed decreased glucose flux through the oxidative arm of the PPP (G6PD flux) (Figure 4d). Despite decreasing glucose flux through G6PD, HIF-1α induced the production of ribose 5-phosphate through the non-oxidative arm of the PPP (Figure 4e).

We investigated the effect of inhibiting HIF-1α on the TKT flux. Cells with constitutive expression of HIF-1α short hairpin RNA (shRNA) exhibited a decrease in the TKT flux,

which was correlated with reduced mRNA levels for all detectable transketolase family genes (Figure 4f and g).

HIF-1α is required for the survival and proliferation of imatinib-resistant cells

HIF-1α activation can promote viability in cells exhibiting a high rate of glucose uptake (Lum *et al.*, 2007). An shRNA expression vector encoding a puromycin-resistance gene and engineered to stably express an shRNA against HIF-1α was transfected into imatinib-resistant cells (Lum *et al.*, 2007). After 10 days of culture, during which the medium containing both imatinib and the selection drug puromycin was replaced every 2-3 days, few cells survived in the cultures transfected with the HIF-1α shRNA expression plasmid while cultures transfected with the control shRNA had undergone a 5-fold expansion (Figure 5a, 5b and Supplemental Figure 6).

Transketolase is a component of HIF-1α-dependent imatinib resistance

Transketolase is a HIF-1α target gene that may contribute to the maintenance of nucleotide biosynthesis in BCR-ABL transformed cells. To test whether the induction of transketolase expression is a component of HIF-1α-mediated imatinib resistance, a plasmid containing an shRNA against Tkt and a puromycin resistance gene was transfected into the imatinib-resistant cells. We chose *Tkt* for knock down in the imatinib-resistant cells because its transcript abundance was over 1,000 fold greater than either *Tktl1* or *Tktl2* (data not shown). After being transfected with either a Tkt shRNA expression plasmid or a plasmid containing a control shRNA, resistant cells (BR) were cultured in the presence of both imatinib and the selection drug puromycin with a change of medium every 2-3 days. After 10 days, cells transfected with control shRNA had expanded 5 fold despite continuous imatinib treatment. In contrast, there were few surviving cells in the cultures transfected with plasmid containing the Tkt shRNA (Figure 5a). This result was specific for the shRNA suppression of Tkt. When imatinib-resistant cells were first stably expressed with human *Tktl1* (transketolase-like 1, a transketolase family gene) that lacks the Tkt shRNA sequence, the transfection of the Tkt shRNA plasmid had no effect on the ability of cells to grow in the presence of both imatinib and puromycin (Figure 5c).

Oxythiamine inhibition of thiamine dependent enzymes restores imatinib sensitivity in imatinib-resistant cells *in vitro*

Oxythiamine is an analog of thiamine, which is a cofactor of transketolase as well as several TCA cycle enzymes. Oxythiamine specifically inhibited glucose-mediated ribose synthesis through the non-oxidative arm of the PPP (TKT flux) (Supplemental Figure 4b and 4c). Furthermore, oxythiamine can selectively inhibit the proliferation of G6PD-deficient CHO cells, which rely exclusively on the non-oxidative PPP for ribose synthesis, without affecting the proliferation of parental CHO cells (Supplemental Figure 7) (Tuttle *et al.*, 1992). In low thiamine medium, neither oxythiamine nor imatinib alone had an inhibitory effect on cell proliferation of murine resistant cells (BR) over a 7-day treatment (Figure 5d and Supplemental Figure 8a). However, combination of oxythiamine and imatinib resulted in an over 90% decrease in cell number. The inhibition of cell proliferation upon combination treatment was also observed in human imatinib-resistant cells (LR) (Figure 5e

and Supplemental Figure 8b). The inhibitory effect of combining oxythiamine and imatinib could be rescued by addition of thiamine to the culture medium (Figure 5d and 5e).

Oxythiamine in combination with imatinib suppresses BCR-ABL expressing tumor growth *in vivo*

A xenograft tumor mouse model was first used to establish that imatinib effectively inhibited BCR-ABL transformed tumor growth *in vivo* (Druker *et al.*, 1996). Therefore, we used a comparable xenograft tumor model to test the efficacy of the combination of imatinib and oxythiamine *in vivo*. Nude mice were subcutaneously injected with either imatinib-sensitive or imatinib-resistant BCR-ABL expressing cells to establish xenografts. Once tumors were established, the mice were randomized to treatments with phosphate-buffer saline (PBS) alone, imatinib alone, oxythiamine alone, or oxythiamine plus imatinib. During the period of treatment, mice treated with oxythiamine (80 mg/kg/day) or imatinib (either 100 mg/kg/day or 200mg/kg/b.i.d.) did not show any observable side effects, such as variations in weight and physical activities. Combining oxythiamine with a higher dose of imatinib (200 mg/kg/day, b.i.d), but not a lower dose of imatinib (100mg/kg/day), resulted in mild weight loss without other observable abnormalities (data not shown). In animals injected with imatinib-resistant cells, single treatment with either a higher dose imatinib (200mg/kg/b.i.d) or oxythiamine had no effect on overall tumor growth over a 2-week period. In contrast, the combination of imatinib with oxythiamine synergistically inhibited the growth of resistant-cell xenografts (Figure 5f). An effect of oxythiamine when combined with imatinib was also observed in imatinib-sensitive tumors. For animals injected with imatinib-sensitive cells, when a subtherapeutic dose of imatinib was administrated (100mg/kg/day), no effect on tumor growth was seen (higher doses resulted in suppression of tumor growth, data not shown). Oxythiamine alone was also ineffective. However, when the suboptimal dose of imatinib was combined with oxythiamine therapy, a significant reduction in tumor growth was observed (Figure 5g), same as shown *in vitro* (Supplemental Figure 9).

Oxythiamine improves the efficacy of imatinib in primary CML cells isolated from patients in the accelerated/blastic phase of the disease

BCR-ABL amplification has been shown in CML patients when the diseases progresses into accelerated/blastic phase and BCR-ABL expressing cells become resistant to imatinib (Barnes *et al.*, 2005a; Gorre *et al.*, 2001) (Supplemental Figure 10). To demonstrate the effect of combining oxythiamine and imatinib on the proliferation of primary CML cells, colony formation was examined for MNCs isolated from two CML patients in the accelerated phase of the disease (supplementary information). Colony formation in both patients was about 50% inhibited with imatinib treatment. Treatment with oxythiamine alone had no significant inhibitory effect. However, when cells were treated with oxythiamine and imatinib, the number of colonies was significantly reduced, compared to that treated with imatinib alone. This inhibition of oxythiamine was specific since the colony formation could be rescued to the level comparable to imatinib treatment alone by the addition of thiamine (Figure 6).

Discussion

The level of BCR-ABL expression increases as tumors progress from the chronic phase (Gorre *et al.*, 2001). Increased BCR-ABL has also been observed when BCR-ABL transformed cells are selected for imatinib resistance *in vitro* (Mahon *et al.*, 2000) (Figure 1). Surprisingly, here we show imatinib-resistant cells displayed an increase in glycolysis but a reduced rate of proliferation. The effect is reminiscent of the effects of HIF-1α induction in cells exhibiting aerobic glycolysis (Lum *et al.*, 2007). We demonstrate that HIF-1α was induced in response to high levels of BCR-ABL expression and was required to maintain the viability of such cells. The observed BCR-ABL induction of HIF-1α appears to lead to a relatively sustained conversion to aerobic glycolysis just as hypoxic induction of HIF-1α leads to sustained anaerobic glycolysis.

Cells with high levels of BCR-ABL expression are at a growth disadvantage in comparison to cells with low levels of BCR-ABL when BCR-ABL-induced glucose metabolism exceeds the capacity of a cell to assimilate or store glucose-derived carbon. BCR-ABL induces increased expression of HIF-1α and glucose uptake. In part, BCR-ABL has been reported to increase HIF-1α through PI3K activation (Mayerhofer *et al.*, 2002). The BCR-ABL induction of HIF-1α redirects glucose metabolism away from mitochondria (Gottschalk *et al.*, 2004). While the induction of HIF-1α in response to excess glucose catabolism (Zhang *et al.*, 2008) or hypoxia (Giuntoli *et al.*, 2006) is cytoprotective, activation of HIF-1α reduces the synthetic capacity of the mitochondria and diverts glucose metabolism away from the oxidative arm of the PPP (Lum *et al.*, 2007). The resulting decrease in the production of fatty acids, TCA-cycle-derived non-essential amino acids, and ribose correlated with a reduced ability to proliferate. Thus, even in transformed cells, there appears to be a level of glucose metabolism that can paradoxically suppress in *cis* the proliferation of a cell.

Most cancer cells depend on *de novo* nucleotide biosynthesis for growth and survival (Zaharevitz *et al.*, 1992). This has been exploited in cancer therapy through the use of inhibitors of dihydrofolate reductase, thymidylate synthase, glutamine phosphoribosylpyrophosphate amidotransferase and adenosine deaminase. Ribose can be produced both in the oxidative and non-oxidative arms of the PPP. This has been interpreted to mean that an effective inhibitor of ribose synthesis would have to block both arms. Such drugs might thus have heightened toxicities for normal cells. Our data suggest that in cells depending on HIF-1α for continuous survival, effective ribose synthesis can only be maintained from the non-oxidative arm of the PPP. This suggests that inhibitors of the non-oxidative PPP may have selective effects in tumors exhibiting constitutive HIF-1α activation. Such a targeted therapeutic use may limit the toxicity for non-transformed cells that retain an intact oxidative arm of the PPP. Consistent with this, oxythiamine, an inhibitor of thiamine dependent enzymes, was found to synergize with imatinib in suppressing the growth and proliferation of BCR-ABL transformed cells *in vitro*. How long such an effect can be sustained in chronically treated cells will require additional study.

In conclusion, our study provides insight into relative imatinib resistance associated with the increased BCR-ABL expression observed in leukemic cells of patients with accelerated

CML. Collectively, the above observations support the hypothesis that the induction of HIF-1α may contribute to the imatinib resistance exhibited by such cells. The ongoing development of HIF-1α inhibitors may soon allow this hypothesis to be tested. The potential ability of HIF-1α induction to reduce the oncogene addiction of BCR-ABL transformed cells may be relevant to other oncogenes that activate the glucose metabolism of transformed cells, and this will need to be explored in future studies.

Materials and Methods

Generation of imatinib resistant cells, cell lines and reagents

All chemicals were from Sigma-aldrich (St. Louis, MO) and all cell culture reagents were from Invitrogen (Carlsbad, CA) unless indicated otherwise.

The BCR-ABL transformed murine hematopoietic BaF3 cell line (BaF3/p210) was established previously (Carroll *et al.*, 1997). To generate imatinib-resistant cells, BaF3/p210 cells were incubated in the presence of imatinib (0.5 or 1 μM) and imatinib-supplemented culture medium was refreshed every 3 days until the outgrowth of a resistant population, after roughly 3 weeks. Isogenic sensitive cells (BS) were maintained at the same passage. Human imatinib resistant LAMA-84-R cell line (LR) was generated and maintained as described previously (Mahon *et al.*, 2000). Imatinib resistant cells were maintained with additional supplementation of either 0.5 μM (BR cells) or 1 μM (LR) imatinib, which was transiently withdrawn from medium for the course of the experiments described in this study. For *in vitro* treatments with oxythiamine, BR cells and LR cells were cultured in F-12 Kaighn's nutrient mixture and McCoy's 5A medium with supplements, respectively.

Human embryonic kidney 293T cell lines transfected with either vector or a non-degradable HIF-1α construct in an inducible system (HIF1A-DPA), Chinese hamster ovary cells (CHO) with or without G6PD deficiency and IL-3 dependent *bax*$^{-/-}$*bak*$^{-/-}$ cells with or without knockdown of *HIF-1α* were described previously (Hu *et al.*, 2003; Lum *et al.*, 2007; Tuttle *et al.*, 1992).

Glucose uptake, quantitative PCR (qPCR), constructs, cell transfection and antibodies

Glucose concentration in the medium was determined as previously described (Lum *et al.*, 2007). Total RNA was isolated using TRIzol Reagent (Invitrogen) and cDNA was prepared using SuperScript II Reverse Transcriptase (Invitrogen). All samples were normalized to β-actin transcript levels. A construct containing human *Tktl1* cDNA was purchased from Invitrogen and cloned into a mammalian expression vector pEF6/MHC (Invitrogen). A construct containing a control short hairpin or a short hairpin RNA targeting mouse *Tkt* was purchased from Open Biosystems (Huntsville, AL). Transfection was performed by nucleofector transfection (Amaxa, Gaithersburg, MD) using program X01 with 3 μg of DNA per 0.3×10^6 cells. Antibodies: c-Abl (Santa Cruz Biotechnology, Santa Cruz, CA), phospho-694-STAT5A/B (Upstate, Temecula, CA), human HIF-1α (BD Biosciences, San Jose, CA), mouse HIF-1α (a gift from Dr. M.C. Simon) and β-actin (Sigma).

Transketolase activity

In vitro transketolase activity was measured as previously described (Chamberlain *et al.*, 1996). Briefly, 3 ×10^6 cells were washed with PBS before being lysed in M-PER cytosolic lysis buffer (Pierce Biotechnology, Rockford, IL), supplemented with protease inhibitor (EDTA free) (Roche) and phosphatase inhibitor cocktail (Sigma). Ten microliter of lysate was used in a 200 μl reaction mixture, containing 100 mM Tris chloride (pH8.0), 15 mM ribose 5-phosphate, 250 μM NADH, 200mU/ml glycerol-3-phosphate dehydrogenase and 2.5U/ml triose phosphate isomerase. The absorbance at 340nm (OD_{340}) was recorded every 10 min on a plate reader (Beckman). The OD difference between 10-minute point and each time point was normalized by protein amount.

^{14}C-glucose incorporation into RNA

Glucose mediated ribose synthesis from the non-oxidative arm and both arms (the oxidative and non-oxidative) of the PPP was estimated by the incorporation of [1-^{14}C]- and [6-^{14}C]-glucose into RNA, respectively (Figure S3A). One to five microcurie of either [1-^{14}C]-glucose (Sigma) or [6-^{14}C]-glucose (GE Healthcare) was added into culture medium and cells were incubated overnight before being harvested for RNA extraction using RNeasy columns (Qiagen).The ratio of RNA CPM ([1-^{14}C]/[6-^{14}C]) was defined as the relative level of RNA synthesized through the non-oxidative arm of the PPP (TKT flux).

$^{14}CO_2$ release

$^{14}CO_2$ release from glucose through either the oxidative arm of the PPP (G6PD flux) or TCA cycle activity was determined by incubating cells in bicarbonate free medium containing either [1-^{14}C]- or [6-^{14}C]-glucose respectively, as previously described (Tuttle *et al.*, 2007). Glucose uptake during the course of experiment was determined and used to normalize CPM.

Establishment of tumors in nude mice for *in vivo* treatment

Xenografts were established in athymic nude male mice (6-8 weeks old; Tarconic) and tumor mass was measured as described previously (Hatzivassiliou *et al.*, 2005). All procedures were approved by the Institutional Animal Care and Use Committee of the University of Pennsylvania.

Colony formation of CML leukemic cells

Cryopreserved MNCs from CML patients were thawed and plated in MethoCult GF$^+$ H4535 media (StemCell Technologies, Vancouver, BC, Canada). Primary cells from CML patients were incubated in 35 mm plates and assessed for colony formation as previously described (Thompson *et al.*, 2007). Imatinib (Im, 5-10 μM), oxythiamine (OT, 1 mM) and/or thiamine (T, 300 μM) treatment was added from the start of the culture.

Supplementary Material

Refer to Web version on PubMed Central for supplementary material.

Acknowledgments

The authors wish to thank members of the Thompson laboratory, especially Tullia Lindsten, Mondira Kundu, Uma Sachdeva and Scott Olejniczak for helpful suggestions during the study and careful critique of the manuscript. We thank Drs. E Buchdunger (Novartis, Basel, Switzerland) for providing imatinib and E.P. Reddy (Temple University, Philadelphia) for providing cell lines expressing either WT or mutant (T315I) form of BCR-ABL. We are grateful to Drs. MC Simon (University of Pennsylvania), JL Riley (University of Pennsylvania) and DA Tuveson (Cancer Research UK Cambridge Research Institute, UK) for providing experimental reagents. This work was supported in part by grants from the NCI and NIH. The authors declare no conflicts of interest or competing financial interests in relationship to this work.

References

Barnes DJ, Palaiologou D, Panousopoulou E, Schultheis B, Yong AS, Wong A, et al. Bcr-Abl expression levels determine the rate of development of resistance to imatinib mesylate in chronic myeloid leukemia. Cancer Res. 2005a; 65:8912–9. [PubMed: 16204063]

Barnes K, McIntosh E, Whetton AD, Daley GQ, Bentley J, Baldwin SA. Chronic myeloid leukaemia: an investigation into the role of Bcr-Abl-induced abnormalities in glucose transport regulation. Oncogene. 2005b; 24:3257–67. [PubMed: 15735728]

Bell EL, Chandel NS. Mitochondrial oxygen sensing: regulation of hypoxia-inducible factor by mitochondrial generated reactive oxygen species. Essays Biochem. 2007; 43:17–27. [PubMed: 17705790]

Carroll M, Ohno-Jones S, Tamura S, Buchdunger E, Zimmermann J, Lydon NB, et al. CGP 57148, a tyrosine kinase inhibitor, inhibits the growth of cells expressing BCR-ABL, TEL-ABL, and TEL-PDGFR fusion proteins. Blood. 1997; 90:4947–52. [PubMed: 9389713]

Chamberlain BR, Buttery JE, Pannall PR. A stable reagent mixture for the whole blood transketolase assay. Ann Clin Biochem. 1996; 33(Pt 4):352–4. [PubMed: 8836396]

Deininger M, Buchdunger E, Druker BJ. The development of imatinib as a therapeutic agent for chronic myeloid leukemia. Blood. 2005; 105:2640–53. [PubMed: 15618470]

Dewar AL, Doherty KV, Hughes TP, Lyons AB. Imatinib inhibits the functional capacity of cultured human monocytes. Immunol Cell Biol. 2005; 83:48–56. [PubMed: 15661041]

Druker BJ, Tamura S, Buchdunger E, Ohno S, Segal GM, Fanning S, et al. Effects of a selective inhibitor of the Abl tyrosine kinase on the growth of Bcr-Abl positive cells. Nat Med. 1996; 2:561–6. [PubMed: 8616716]

Giuntoli S, Rovida E, Barbetti V, Cipolleschi MG, Olivotto M, Dello Sbarba P. Hypoxia suppresses BCR/Abl and selects imatinib-insensitive progenitors within clonal CML populations. Leukemia. 2006; 20:1291–3. [PubMed: 16710305]

Gorre ME, Mohammed M, Ellwood K, Hsu N, Paquette R, Rao PN, et al. Clinical resistance to STI-571 cancer therapy caused by BCR-ABL gene mutation or amplification. Science. 2001; 293:876–80. [PubMed: 11423618]

Gottschalk S, Anderson N, Hainz C, Eckhardt SG, Serkova NJ. Imatinib (STI571)-mediated changes in glucose metabolism in human leukemia BCR-ABL-positive cells. Clin Cancer Res. 2004; 10:6661–8. [PubMed: 15475456]

Gumireddy K, Baker SJ, Cosenza SC, John P, Kang AD, Robell KA, et al. A non-ATP-competitive inhibitor of BCR-ABL overrides imatinib resistance. Proc Natl Acad Sci U S A. 2005; 102:1992–7. [PubMed: 15677719]

Gupte SA, Wolin MS. Hypoxia promotes relaxation of bovine coronary arteries through lowering cytosolic NADPH. Am J Physiol Heart Circ Physiol. 2006; 290:H2228–38. [PubMed: 16415080]

Haseloff RF, Krause E, Bigl M, Mikoteit K, Stanimirovic D, Blasig IE. Differential protein expression in brain capillary endothelial cells induced by hypoxia and posthypoxic reoxygenation. Proteomics. 2006; 6:1803–9. [PubMed: 16447158]

Hatzivassiliou G, Zhao F, Bauer DE, Andreadis C, Shaw AN, Dhanak D, et al. ATP citrate lyase inhibition can suppress tumor cell growth. Cancer Cell. 2005; 8:311–21. [PubMed: 16226706]

Hu CJ, Wang LY, Chodosh LA, Keith B, Simon MC. Differential roles of hypoxia-inducible factor 1alpha (HIF-1alpha) and HIF-2alpha in hypoxic gene regulation. Mol Cell Biol. 2003; 23:9361–74. [PubMed: 14645546]

Katz J, Rognstad R. The labeling of pentose phosphate from glucose-14C and estimation of the rates of transaldolase, transketolase, the contribution of the pentose cycle, and ribose phosphate synthesis. Biochemistry. 1967; 6:2227–47. [PubMed: 6049456]

Keeshan K, Mills KI, Cotter TG, McKenna SL. Elevated Bcr-Abl expression levels are sufficient for a haematopoietic cell line to acquire a drug-resistant phenotype. Leukemia. 2001; 15:1823–33. [PubMed: 11753601]

Khorashad JS, Anand M, Marin D, Saunders S, Al-Jabary T, Iqbal A, et al. The presence of a BCR-ABL mutant allele in CML does not always explain clinical resistance to imatinib. Leukemia. 2006; 20:658–63. [PubMed: 16467863]

Kim JW, Tchernyshyov I, Semenza GL, Dang CV. HIF-1-mediated expression of pyruvate dehydrogenase kinase: a metabolic switch required for cellular adaptation to hypoxia. Cell Metab. 2006; 3:177–85. [PubMed: 16517405]

Kominsky DJ, Klawitter J, Brown JL, Boros LG, Melo JV, Eckhardt SG, et al. Abnormalities in glucose uptake and metabolism in imatinib-resistant human BCR-ABL-positive cells. Clin Cancer Res. 2009; 15:3442–50. [PubMed: 19401345]

Kress S, Stein A, Maurer P, Weber B, Reichert J, Buchmann A, et al. Expression of hypoxia-inducible genes in tumor cells. J Cancer Res Clin Oncol. 1998; 124:315–20. [PubMed: 9692838]

Lum JJ, Bui T, Gruber M, Gordan JD, DeBerardinis RJ, Covello KL, et al. The transcription factor HIF-1alpha plays a critical role in the growth factor-dependent regulation of both aerobic and anaerobic glycolysis. Genes Dev. 2007; 21:1037–49. [PubMed: 17437992]

Mahon FX, Deininger MW, Schultheis B, Chabrol J, Reiffers J, Goldman JM, et al. Selection and characterization of BCR-ABL positive cell lines with differential sensitivity to the tyrosine kinase inhibitor STI571: diverse mechanisms of resistance. Blood. 2000; 96:1070–9. [PubMed: 10910924]

Mayerhofer M, Valent P, Sperr WR, Griffin JD, Sillaber C. BCR/ABL induces expression of vascular endothelial growth factor and its transcriptional activator, hypoxia inducible factor-1alpha, through a pathway involving phosphoinositide 3-kinase and the mammalian target of rapamycin. Blood. 2002; 100:3767–75. [PubMed: 12393646]

Modi H, McDonald T, Chu S, Yee JK, Forman SJ, Bhatia R. Role of BCR/ABL gene-expression levels in determining the phenotype and imatinib sensitivity of transformed human hematopoietic cells. Blood. 2007; 109:5411–21. [PubMed: 17347407]

O'Hare T, Corbin AS, Druker BJ. Targeted CML therapy: controlling drug resistance, seeking cure. Curr Opin Genet Dev. 2006; 16:92–9. [PubMed: 16343892]

Pan Y, Mansfield KD, Bertozzi CC, Rudenko V, Chan DA, Giaccia AJ, et al. Multiple factors affecting cellular redox status and energy metabolism modulate hypoxia-inducible factor prolyl hydroxylase activity in vivo and in vitro. Mol Cell Biol. 2007; 27:912–25. [PubMed: 17101781]

Papandreou I, Cairns RA, Fontana L, Lim AL, Denko NC. HIF-1 mediates adaptation to hypoxia by actively downregulating mitochondrial oxygen consumption. Cell Metab. 2006; 3:187–97. [PubMed: 16517406]

Pelicano H, Xu RH, Du M, Feng L, Sasaki R, Carew JS, et al. Mitochondrial respiration defects in cancer cells cause activation of Akt survival pathway through a redox-mediated mechanism. J Cell Biol. 2006; 175:913–23. [PubMed: 17158952]

Sherbenou DW, Druker BJ. Applying the discovery of the Philadelphia chromosome. J Clin Invest. 2007; 117:2067–74. [PubMed: 17671641]

Thompson JE, Conlon JP, Yang X, Sanchez PV, Carroll M. Enhanced growth of myelodysplastic colonies in hypoxic conditions. Exp Hematol. 2007; 35:21–31. [PubMed: 17198870]

Tuttle SW, Maity A, Oprysko PR, Kachur AV, Ayene IS, Biaglow JE, et al. Detection of reactive oxygen species via endogenous oxidative pentose phosphate cycle activity in response to oxygen concentration: implications for the mechanism of HIF-1alpha stabilization under moderate hypoxia. J Biol Chem. 2007; 282:36790–6. [PubMed: 17666400]

Tuttle SW, Varnes ME, Mitchell JB, Biaglow JE. Sensitivity to chemical oxidants and radiation in CHO cell lines deficient in oxidative pentose cycle activity. Int J Radiat Oncol Biol Phys. 1992; 22:671–5. [PubMed: 1544835]

Zaharevitz DW, Anderson LW, Malinowski NM, Hyman R, Strong JM, Cysyk RL. Contribution of de-novo and salvage synthesis to the uracil nucleotide pool in mouse tissues and tumors in vivo. Eur J Biochem. 1992; 210:293–6. [PubMed: 1446677]

Zhang H, Bosch-Marce M, Shimoda LA, Tan YS, Baek JH, Wesley JB, et al. Mitochondrial autophagy is an HIF-1-dependent adaptive metabolic response to hypoxia. J Biol Chem. 2008; 283:10892–903. [PubMed: 18281291]

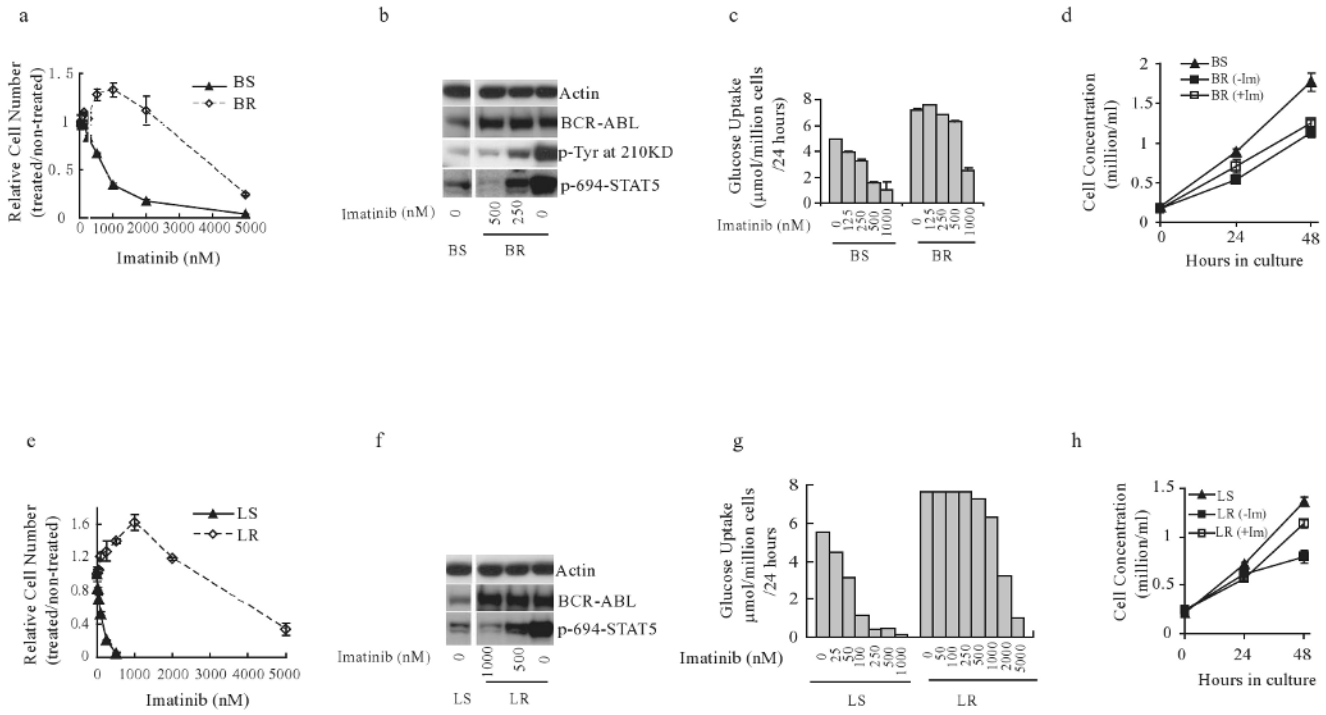

Figure 1. Imatinib-resistant cells display upregulated BCR-ABL protein level, increased glucose uptake, and reduced cell proliferation

(a) to (d), murine imatinib-sensitive (BS) and imatinib-resistant cells (BR). (e) to (h), human imatinib-sensitive (LS) and imatinib-resistant cells (LR). For a to d, equivalent results were also obtained with an independently derived cell line.

(a) and (e), Cells were treated with imatinib for 2 days and cell density was determined by trypan blue staining. Relative cell number (mean ± SD) of triplicate samples of a representative experiment is shown.

(b) and (f), Western-blot analysis of the BCR-ABL signaling pathway. Cells were treated with imatinib overnight. Thirty μg of total protein lysate was loaded and immunoblotted for indicated proteins.

(c) and (g), Glucose uptake. Cells were treated with imatinib overnight and replated at the density of 0.5×10^6/ml in refreshed medium for 24 hours. Glucose content in medium supernatants was measured. Glucose uptake = (glucose in the medium before the treatment – glucose in the medium after imatinib treatment). Experiment was done in triplicate, and shown is mean glucose uptake (μmol) /10^6 cells/24 hours (± SD) of a representative experiment.

(d) and (h), Cell proliferation. Cells were grown in the absence (-Im) or presence (+Im) of imatinib (Im, 0.5 μM for BR and 1 μM for LR) at a starting concentration of 0.2×10^6/ml in triplicate and counted at 0, 24-hour and 48-hour points, respectively. Shown is mean cell concentration (10^6/ml) ± SD of a representative experiment.

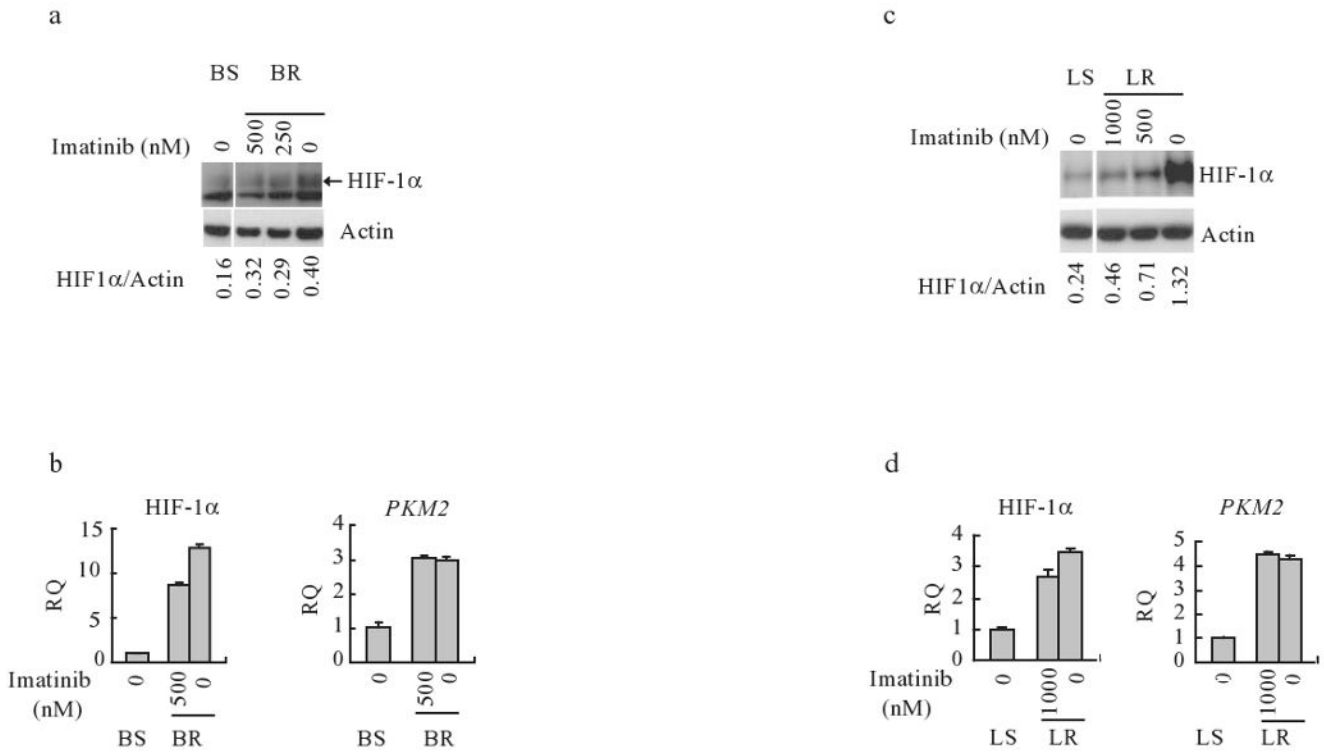

Figure 2. Induction of HIF-1α and its targets in imatinib-resistant cells

Cells were grown in the absence or presence of varying concentrations of imatinib overnight before being harvested for protein or RNA extraction. (a) and (b), murine imatinib-sensitive (BS) and imatinib-resistant cells (BR). (c) and (d), human imatinib-sensitive (LS) and imatinib-resistant cells (LR). The data shown is representative of at least 3 experiments for each cell line. (a) and (c), Western blotting for HIF-1α protein levels. Relative levels of HIF-1α compared to endogenous actin were quantitated and shown below. (b) and (d), Quantitative PCR (qPCR) analysis was used to determine transcript levels. Shown is relative quantity (RQ)±SD.

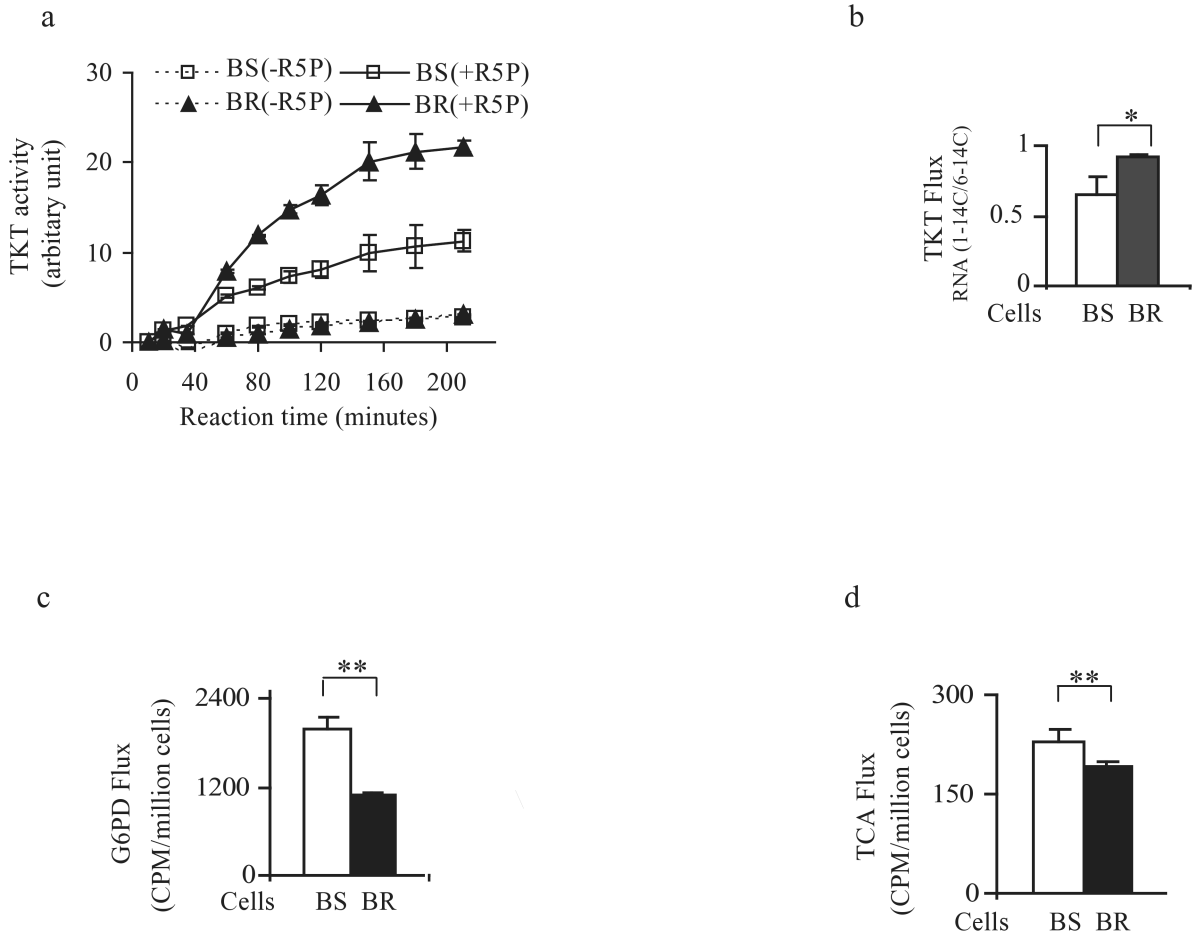

Figure 3. Imatinib-resistant cells demonstrate a relative increase in glucose flux through the non-oxidative arm of the PPP for ribose synthesis

(a), *In vitro* transketolase activity. Transketolase activity (TKT activity) was determined as described in Materials and Methods. Shown is TKT activity (arbitrary units) ± SD in the absence (-R5P) or presence (+R5P) of ribose 5-phosphate (R5P). BS, imatinib-sensitive cells; BR, imatinib-resistant cells.

(b), ^{14}C-glucose incorporation into RNA. Experiment was performed as described in Materials and Methods. CPM ratio ([1-^{14}C]/ [6-^{14}C]) was defined as relative transketolase flux (TKT flux). Shown is relative TKT flux ±SEM. * indicates $p<0.05$ as determined by unpaired Student t-test.

(c), $^{14}CO_2$ release from the oxidative arm of the PPP (G6PD flux). The experiment was performed in triplicate. Shown is CPM for G6PD flux (/10^6 cells) ± SD. ** indicates $p<0.01$ as determined by unpaired Student t-test.

(d), $^{14}CO_2$ release from the TCA cycle. Experiment was done in triplicate. Shown is CPM for TCA flux (/10^6 cells) ± SD. ** indicates $p<0.01$ as determined by unpaired Student t-test.

Open bar, imatinib-sensitive cells (BS); black bar, imatinib-resistant cells (BR).

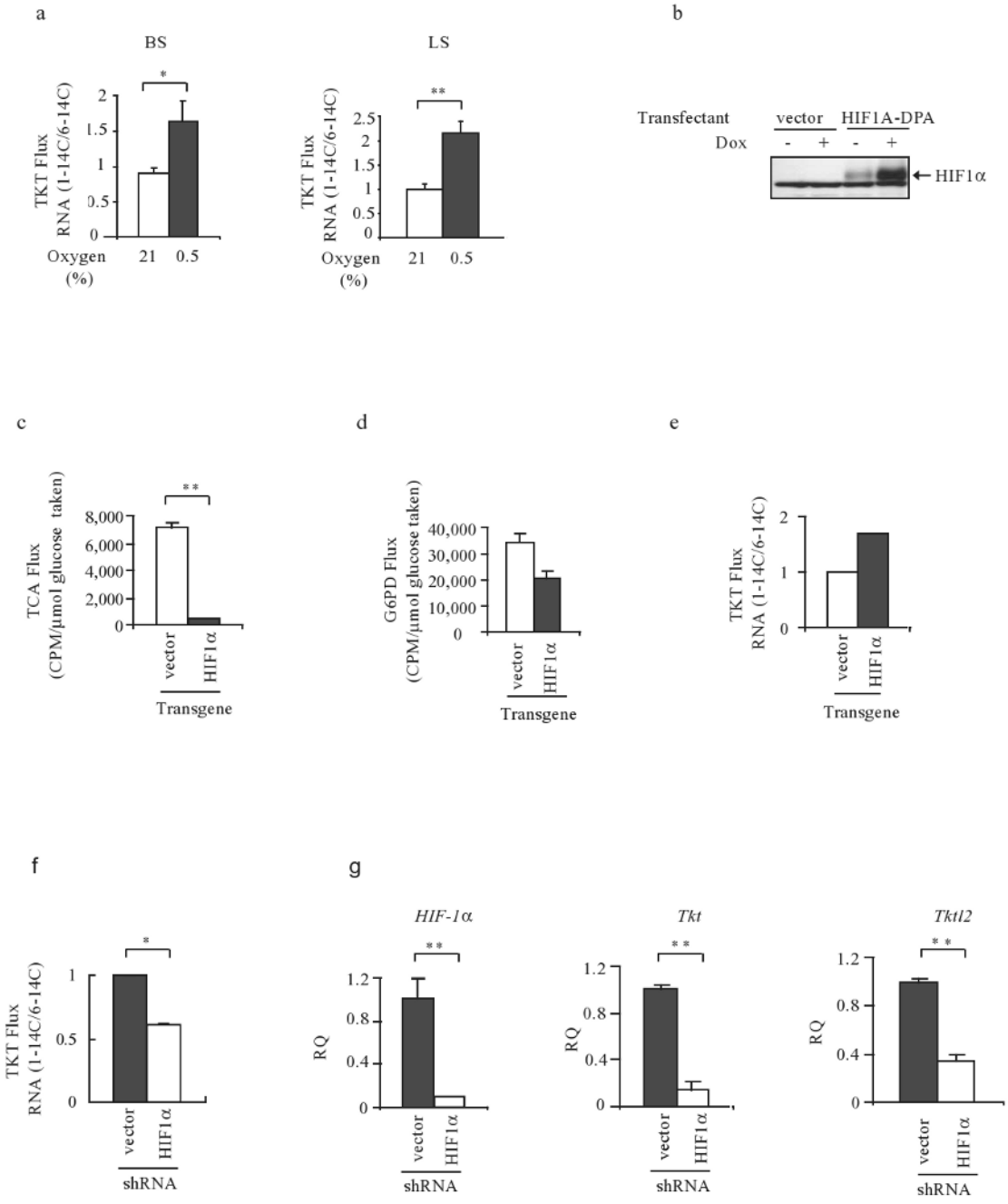

Figure 4. HIF-1α induces glucose flux towards the non-oxidative arm of the PPP for ribose synthesis

a, Hypoxic conditions switch BCR-ABL transformed cells more dependent on non-oxidative PPP for ribose synthesis. Imatinib-sensitive cells (BS and LS) were cultured under hypoxic condition (0.5% O_2 level) for two days before cells were replated and ^{14}C-glucose incorporation into RNA was performed as described in Materials and Methods. Shown is relative TKT flux ±SEM. * indicates $p<0.05$ and ** indicates $p<0.01$, as determined by unpaired Student *t*-test.

b to e, Experiments were performed in 293T cells stably transfected with a non-degradable HIF-1α construct in an inducible system (Hu *et al.*, 2003). (b), Induction of HIF-1α with 1 μg/ml doxycycline (Dox) for 2 days is shown by Western-blot analysis. The non-specific band under the HIF-1α protein signal is served as a loading control. (c), $^{14}CO_2$ release through the TCA cycle using [6-^{14}C]-glucose upon HIF-1α induction. Shown is CPM for TCA flux (normalized by glucose uptake) ± SD. ** indicates $p<0.05$, as determined by unpaired Student *t*-test. (d), $^{14}CO_2$ release through G6PD (the oxidative arm of the PPP) using [1-^{14}C]-glucose upon HIF-1α induction. Actual flux through G6PD was corrected by CO_2 release from [6-^{14}C]-glucose. Shown is CPM for G6PD flux (normalized by glucose uptake) ± SD. (e), ^{14}C-glucose incorporation into RNA upon HIF-1α induction. Experiment was performed as described in Materials and Methods. Shown is relative TKT flux (RNA [1-^{14}C]/ [6-^{14}C]).

f and g, Experiments were performed in IL3-dependent *bax* $^{(-/-)}$ *bak* $^{(-/-)}$ cells stably transfected with either a HIF-1α shRNA vector (HIF-1α) or a control vector (vector) (Lum *et al.*, 2007). (f), ^{14}C-glucose incorporation into RNA upon HIF-1α knockdown. Shown is the relative TKT flux. The inhibition of Tkt flux was also observed in an independent cell clone with stable knockdown of HIF-1α (data not shown). (g), qPCR analysis demonstrates the downregulation of transketolase genes in cells expressing a stable shRNA against HIF-1α. Shown is RQ±SD. *Tkt*, transketolase; *Tktl2*, transketolase like 2. *Tktl1* (transketolase like 1) was undetectable in these cells. * indicates $p<0.05$ and ** indicates $p<0.01$, as determined by unpaired Student *t*-test.

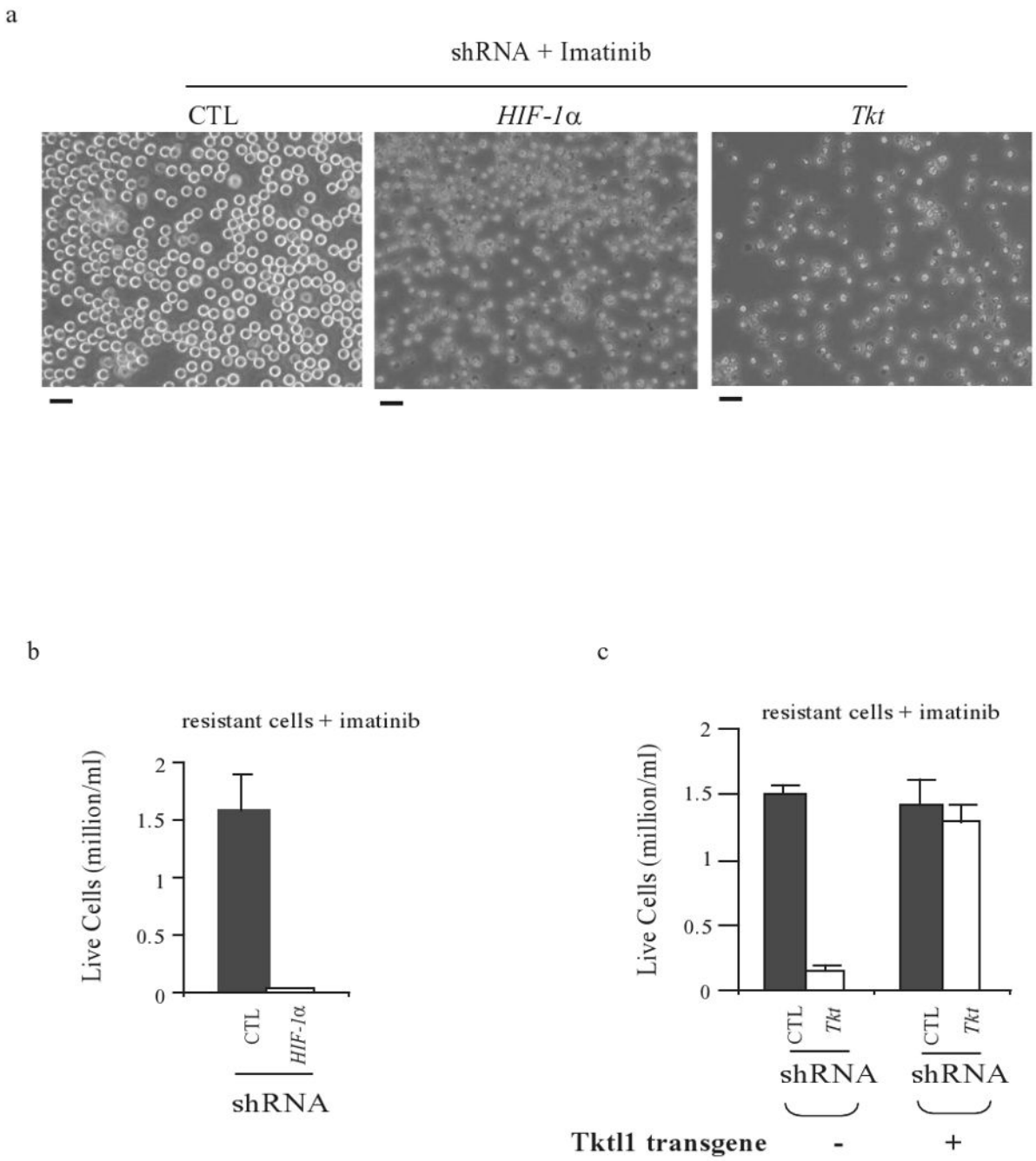

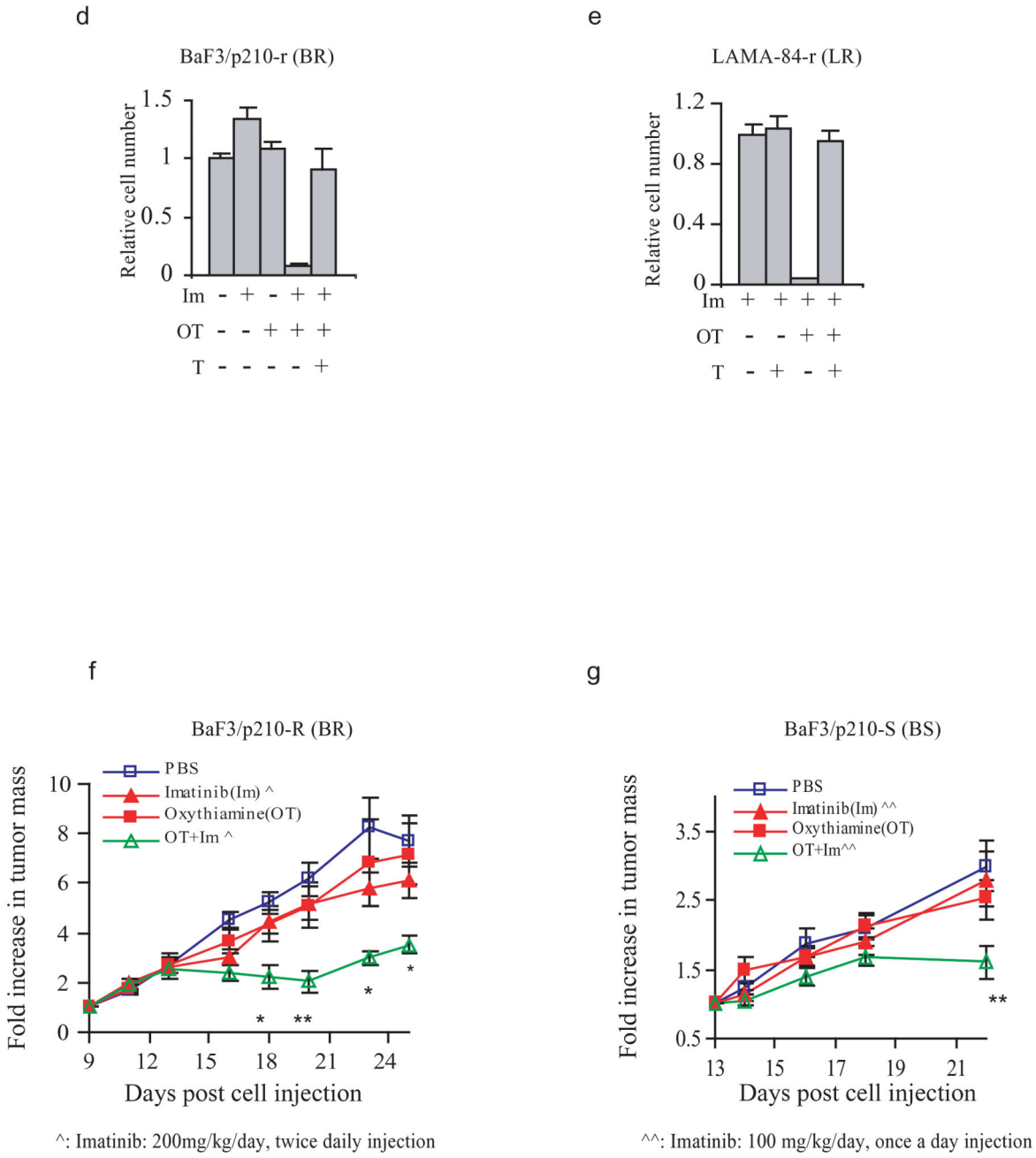

Figure 5. Inhibition of the non-oxidative nucleotide synthesis restores imatinib sensitivity in resistant cells *in vitro and in vivo*

a-c, BR cells were transfected with constructs containing either control shRNA (CTL), an shRNA against HIF-1α (HIF-1α) (Lum *et al.*, 2007) or an shRNA against Tkt (Tkt) and cultured in the presence of imatinib (0.5 μM) and the selection drug puromycin (2 μg/ml), with a change of medium every 2-3 days. After 10 days of puromycin selection, cells are shown by bright-field microscopy (a) and live cell counts were performed (b and c) from a representative experiment. Scale bars = 20 μm.

d, The transketolase inhibitor, oxythiamine, in combination with imatinib suppressed cell proliferation in murine imatinib-resistant BR cells *in vitro*. Cells were plated at a density of 0.15×10^6/ml on day 0 and diluted every 2-3 days with fresh medium. Following 7 days of culture, viable cells were counted and shown is the relative cell number compared to untreated cells (± SD) from a representative experiment. Oxythiamine (OT) was added to cultures at 300 μM, imatinib (Im) was added at 0.5 μM and thiamine (T) was added at 50 μM as indicated.

e, Oxythiamine in combination with imatinib suppressed cell proliferation in human imatinib-resistant LR cells *in vitro*. Cells were plated at a density of 0.3×10^6/ml on day 0 and diluted every 2 days with fresh medium. Following 6 days of culture, viable cells were counted and shown is the relative cell number compared to untreated cells (± SD) from a representative experiment. Oxythiamine (OT) was added to cultures at 1 mM, imatinib (Im) was added at 1 μM and thiamine (T) was added at 150 μM as indicated.

f and g, Combination of oxythiamine and imatinib suppresses BCR-ABL expressing tumor growth *in vivo*. (f), Established tumors derived from imatinib-resistant cells (BR) were treated with PBS (n=5), oxythiamine (80mg/kg/day, once daily) (n=6), imatinib (200mg/kg/day, twice daily) (n=9), or oxythiamine plus imatinib (OT+Im) (n=6) beginning 9 days after tumor initiation with 3×10^6 cells, with the average tumor size around 100 mm^3. Treatment was performed for 17 days by intraperitoneal injection. Shown is the relative increase in tumor mass ± SEM. ** indicates $p < 0.01$ on day 20 and * indicates $p<0.05$ on days 18, 23, 25 between combination treatment group and any other treatment group, as determined by unpaired Student t-test. Effect of combining oxythiamine and imatinib *via* oral administration on tumor growth was also evaluated and similar result was obtained (data not shown). (g), Established tumors derived from imatinib-sensitive cells (BS) were treated with PBS (n=4), oxythiamine (80mg/kg/day) (n=6), imatinib (100mg/kg/day) (n=6), or oxythiamine plus imatinib (OT+Im) (n=5) beginning 13 days after tumor initiation with 1.5×10^6 cells, with the average tumor size around 250 mm^3. Treatment was performed once daily for 9 days *via* oral administration. Shown is the relative increase in tumor mass ± SEM. ** indicates $p < 0.01$ on day 22 between combination treatment group and any other treatment group, as determined by unpaired Student t-test.

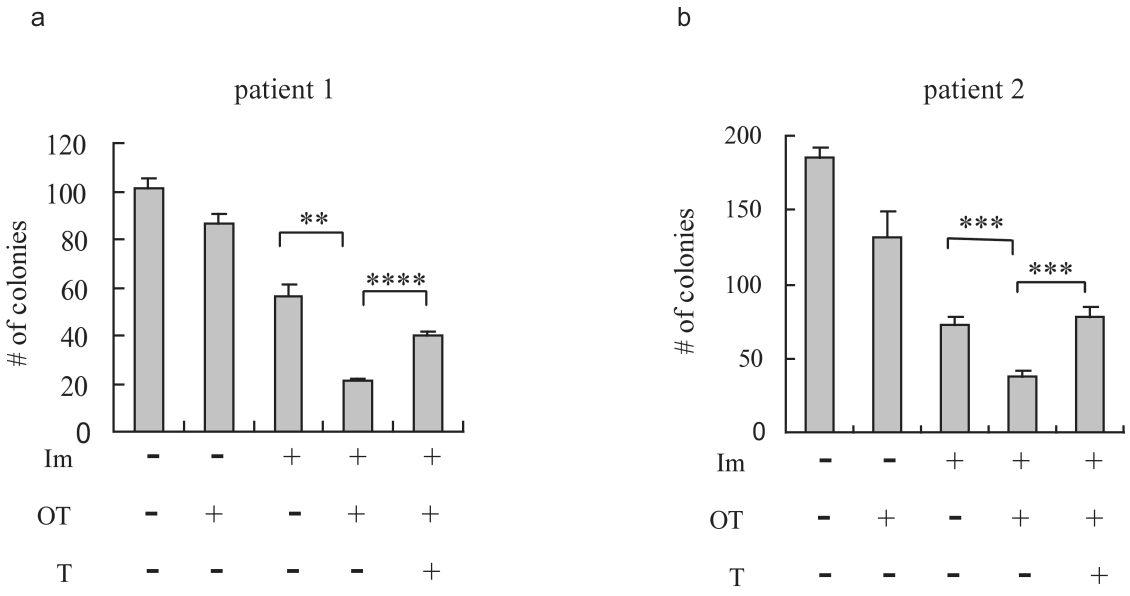

Figure 6. Oxythiamine enhances the efficacy of imatinib in primary CML cells isolated from patients in the accelerated/blastic phase of the disease

MNCs from two patients at the accelerated phase of the disease were harvested and plated for the colony formation as described in Materials and Methods, with indicated treatments. Two weeks later, colonies were counted. The experiment was performed in triplicate and shown is the averaged number of colonies from each plate ± SEM. ** indicates $p<0.01$, *** indicates $p<0.001$ and **** indicates $p<0.0001$, as determined by unpaired Student t-test. Oxythiamine (OT), imatinib (Im) and thiamine (T) were added as indicated.